Catal Lett (2013) 143:1108–1115
DOI 10.1007/s10562-013-1117-0

CO Oxidation Over Monolayer Manganese Oxide Films on Pt(111)

Y. Martynova · M. Soldemo · J. Weissenrieder · S. Sachert · S. Polzin · W. Widdra · S. Shaikhutdinov · H.-J. Freund

Received: 14 August 2013 / Accepted: 22 September 2013 / Published online: 12 October 2013

Abstract Ultrathin manganese oxide films grown on Pt(111) were examined in the low temperature CO oxidation reaction at near atmospheric pressures. Structural characterization was performed by X-ray photoelectron spectroscopy, Auger electron spectroscopy, high-resolution electron energy loss spectroscopy, and temperature programmed desorption. The results show that the reactivity of MnO_x ultrathin films is governed by a weakly bonded oxygen species, which may even be formed at low oxygen pressures ($\sim 10^{-6}$ mbar). For stable catalytic performance at realistic conditions the films required highly oxidizing conditions ($CO:O_2 < 1:10$), otherwise the films dewetted, ultimately resulting in the catalyst deactivation. Comparison with other thin films on Pt(111) shows, that the desorption temperature of weakly bonded oxygen species can be used as a benchmark for its activity in this reaction.

Keywords Ultrathin oxide films · Manganese oxide · CO oxidation

1 Introduction

Ultrathin oxide films, either formed on metal surfaces in oxygen atmosphere or grown on another metal substrate, have recently drawn attention as interesting catalytic materials for the oxidation reactions, particularly in CO oxidation at low temperatures [1–8]. The experimental results showed that the active surface under net oxidizing reaction conditions is often represented by an O–M–O trilayer (M = Fe, Ir, Ru, Rh, Pd) that reveals much higher activity than the metal surface [9–13]. It has also been noted that the reaction had to be performed in excess of oxygen in the gas phase to maintain the active structure of the film, which otherwise dewets and/or becomes partially reduced. In the case of FeO(111) film on Pt(111), dewetting was shown to result in the catalysts deactivation [7]. At a variance, for ZnO(0001) partially covered Pt(111) films the interface showed a much higher reaction rate than observed for the closed films [14].

In the continuation of these studies, we addressed here the reactivity of manganese oxide films on Pt(111). Mn neighbors Fe in the periodic table, and therefore it would be interesting to compare the reactivities of these two metals oxides on the same support. Preparation of MnO_x thin films on Pt(111) has recently been developed [15–17]. It is well-established now that the thinnest well-ordered MnO film, prepared by physical vapor deposition, grows as a non-polar, [001]-oriented MnO monolayer exhibiting an uniaxial reconstruction, ultimately resulting in a complex (19×1) superstructure [15]. Based on high-resolution electron energy loss spectroscopy (HREELS) study, the

Electronic supplementary material The online version of this article (doi:10.1007/s10562-013-1117-0) contains supplementary material, which is available to authorized users.

Y. Martynova · S. Shaikhutdinov (✉) · H.-J. Freund
Abteilung Chemische Physik, Fritz-Haber-Institut der Max-Planck-Gesellschaft, 14195 Berlin, Germany
e-mail: shaikhutdinov@fhi-berlin.mpg.de

M. Soldemo · J. Weissenrieder
Material Physics, KTH Royal Institute of Technology, 16440 Kista, Sweden

S. Sachert · S. Polzin · W. Widdra
Institute of Physics, Martin-Luther-Universität Halle-Wittenberg, 06120 Halle, Germany

W. Widdra
Max-Planck-Institut für Mikrostrukturphysik, 06120 Halle, Germany

thicker films showed a complex behavior, depending on the preparation conditions [16]. The films of ca. 1.3 nm in thickness, grown by chemical vapor deposition, exposed a MnO(111) surface as shown by low-energy electron diffraction (LEED) [17]. Based on angle scanned X-ray photoelectron diffraction study, it was proposed that this film is terminated by a O–Mn–O trilayer structure, i.e. the same structural motif as observed for the FeO(111) monolayer films at elevated oxygen pressures [10].

Manganese oxides naturally crystallize in MnO, Mn_3O_4, Mn_2O_3 and MnO_2 phases, with some like birnessite being non-stoichiometric. Catalytic properties of MnO_x in oxidation reactions are commonly discussed in terms of multivalency of Mn that facilitates supplying lattice oxygen to reactive ad-species. Aimed at a fundamental understanding of the reactivity of MnO_x surfaces many publications focused on the epitaxial growth and structural properties of MnO_x thin films. Besides the already mentioned film growth on Pt(111), well-ordered films could be grown on Ag(001) [18], Pd(100) [19], and Rh(100) [20], to name a few. Very recently, a monolayer film with O–Mn–O structure was reported for Rh(111) [21].

In this work, we address the structure and reactivity of ultrathin MnO_x films in CO oxidation. Ex situ structural characterization of the films by LEED, HREELS, Auger electron spectroscopy (AES), and temperature programmed desorption (TPD), was complemented by in situ high-pressure X-ray photoelectron spectroscopy (HP-XPS) with synchrotron radiation.

2 Experimental

The experiments were performed in three different UHV chambers. The first chamber (at FHI, Berlin) is equipped with LEED optics combined with AES for sample characterization and a differentially-pumped quadrupole mass spectrometer (QMS) for TPD studies. The chamber houses a small (30 ml) gold-plated HP cell connected to a gas chromatograph (GC) for the reactivity measurements as described elsewhere [7]. A double-side polished Pt(111) single crystal was spot welded to the two Ta wires used for resistive heating and also for cooling by filling a manipulator rod with liquid nitrogen. The temperature was measured by a type K thermocouple spot-welded to the edge of the crystal. The HP cell is sealed via a Viton O-ring and then filled with CO and O_2 in the mbar pressure range (He balance to 1 bar) at 300 K. Gas intermixing is achieved with a circulating membrane pump.

The similarly prepared oxide films on Pt(111) were studied at the synchrotron radiation facility MAX-lab (beamline I511-1), Lund University, Sweden. The preparation UHV chamber of the endstation [22] was equipped with LEED. A load-lock was used for sample transfer without breaking vacuum. The main chamber houses a hemispherical analyzer for XPS and a HP cell that allows catalytic reactivity measurements at pressures up to several mbar. The monochromated synchrotron radiation enters the cell via a Si_3N_4 membrane window while the electrons escape to the analyzer through an aperture (1 mm in diameter) placed a few millimeters away from the crystal surface. The crystal is heated in the preparation chamber by direct electron bombardment of the sample plate. In the HP cell, the heating is provided through electron bombardment of the reactor wall. The sample temperature is measured both by a type K thermocouple and a pyrometer. The reaction was carried in a flow regime and monitored by QMS.

The third chamber (at MLU Halle-Wittenberg) is equipped with a HREEL-spectrometer (Delta 05, from Specs), LEED, and TPD facilities. If not stated otherwise the HREEL-spectra were recorded at a sample temperature of 85 K using electron kinetic energies of 4 eV in specular conditions with a total scattering angle of 120°. TPD spectra were measured with QMS using Feulner cup [23].

In all three chambers, clean metallic Pt(111) surfaces were prepared by cycles of Ar^+ ion sputtering and annealing in UHV or O_2 ambient. The manganese oxide films were prepared by Mn vapor deposition using electron beam assisted evaporators in O_2 ambient ($<10^{-7}$ mbar). The film coverage was determined by CO titration of the Pt surface using TPD.

3 Results and Discussion

3.1 Preparation and Structural Characterization

The deposition of Mn atoms on a Pt(111) surface at 375 K in 5×10^{-8} mbar O_2 leads to the formation of a MnO(100)-(19 × 1) film. Its long-range order is further improved by UHV annealing at 600–750 K as judged by LEED. The film is characterized by a sharp Fuchs–Kliewer phonon at 365 cm^{-1}, shown in Fig. 1a for a coverage of ~0.3 monolayers (ML) as measured by CO TPD. This phonon mode is attributed to the collective vertical vibration of the oxygen sub-lattice against the Mn sub-lattice [15]. Subsequent annealing to 750 K in 10^{-6} mbar O_2 for 15 min converts the film into a new, so-called "oxygen-rich" structure that shows no longer the phonon at 365 cm^{-1}, but new features at 478, 583 and 721 cm^{-1} (Fig. 1b). The energy loss at 478 cm^{-1} can be straightforwardly assigned to the frustrated translation of atomic oxygen present on the uncovered Pt(111) surface due to the sample cooling in the oxygen atmosphere. This peak diminishes at increasing film coverage, and can be removed

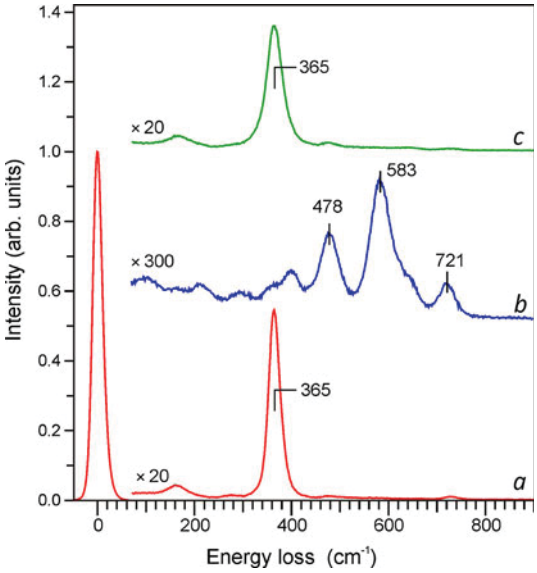

Fig. 1 HREEL spectra of a 0.3 ML MnO ultrathin film on Pt(111) grown at 375 K in 5×10^{-8} mbar O_2 (*a*) and after oxidation at 750 K in 10^{-6} mbar O_2 for 15 min (*b*). Spectrum (*c*) shows the film *b* after six cycles of CO adsorption (200 L at 85 K) and subsequent annealing to 585 K

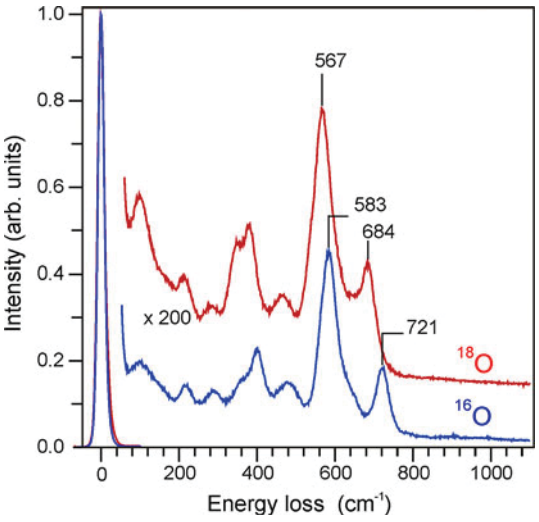

Fig. 2 HREEL spectra of "oxygen-rich" MnO_x films prepared with $^{16}O_2$ (*bottom*) and $^{18}O_2$ (*top*), respectively. The film coverage is 0.8 ML

by heating to 700 K in UHV without changing the manganese oxide related vibrations. However, upon heating to the temperatures above 1050 K, the film is fully transformed back to a well-ordered (19 × 1) structure as judged by LEED and HREELS.

The vibrational spectra of the O-rich film are shown in more details in Fig. 2 for 0.8 ML films prepared either in an $^{16}O_2$ or an $^{18}O_2$ atmosphere. The films show the characteristic phonon modes at 583 and 721 cm^{-1} in the ^{16}O containing film, which red-shift by 16 and 37 cm^{-1},

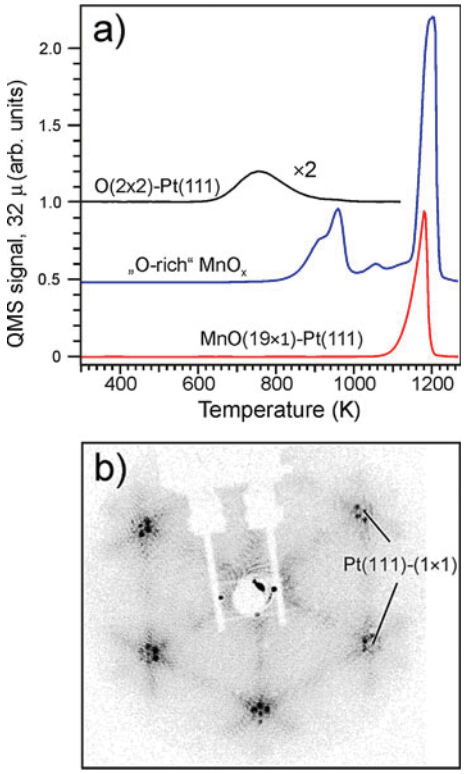

Fig. 3 **a** Oxygen (32 amu) desorption traces of the MnO(100)-(19 × 1) film (*bottom*, *red*), the "O-rich" MnO_x film on Pt(111) (*middle*, *blue*), and the O(2 × 2)–Pt(111) phase (*top*, *black*). The heating rate is 5 K s^{-1} for all spectra. **b** LEED pattern of the "O-rich" MnO_x film prepared by oxidation of a MnO(100)-(19 × 1) film at 750 K in 10^{-6} mbar O_2 for 15 min (coverage 0.9 ML, electron energy 100 eV)

respectively, for the ^{18}O containing oxide film. The weaker low frequency modes around 360 and 400 cm^{-1} also show a notable isotopic shift upon $^{16}O/^{18}O$ substitution. We assign, therefore, the modes at 583 and 721 cm^{-1} to the dipole-active Fuchs–Kliewer phonon-polaritons, whereas the low frequency modes are assigned to microscopic phonon modes as discussed in the details for the case of NiO(100) thin films on Ag(100) [24].

The oxygen desorption states in the O-rich MnO_x films were studied by TPD (Fig. 3a). For MnO(100)–(19 × 1) oxygen desorption takes place in a single peak at 1175 K, whereas the O-rich MnO_x film exhibits three additional peaks between 850 and 1100 K. The amount of oxygen released during thermal decomposition was calibrated vs a well-known O(2 × 2)-Pt(111) surface possessing an 0.25 ML of oxygen. This measured stoichiometry of the O-rich MnO_x film was around Mn:O = 0.4 (±0.15), that is close to a MnO_2 compositional stoichiometry.

The film reconstruction into the O-rich phase is also accompanied by changes in LEED, which are most visible for the films at high coverage as depicted in Fig. 3b, where six inequivalent spots surround the hexagonal

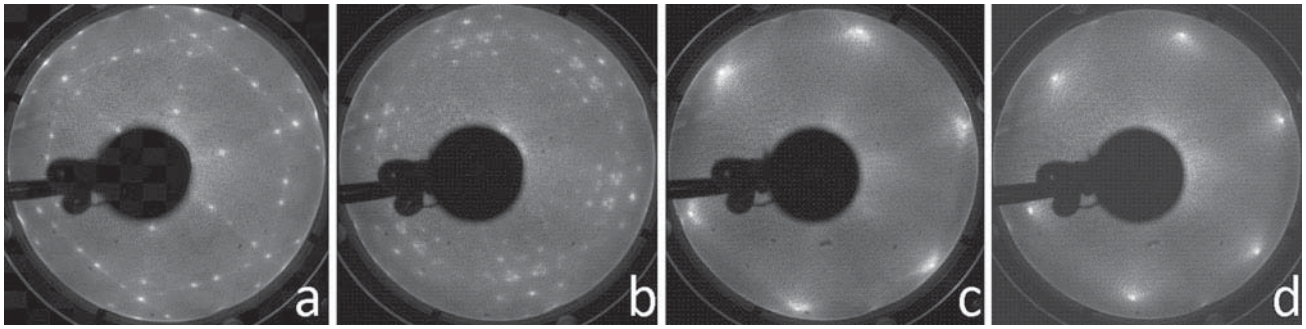

Fig. 4 LEED patterns (at 70 eV) of monolayer manganese oxide films grown on Pt(111): MnO(19 × 1)–Pt(111) (**a**), a MnO_x phase formed by oxidation in 10^{-6} mbar at 850 K (**b**), a film prepared by oxidation at 10^{-4} mbar O_2 at 700 K (**c**). Shown in **d** are the films (**a**, **b**) exposed to 20 mbar O_2 at 450 K

Pt(111)-(1 × 1) spots. Such a Moire-like pattern is indicative for a hexagonal (111)-oriented film with a ~7 % lattice mismatch with respect to the Pt(111) substrate. Taken all these findings together, we have tentatively proposed that the O-rich film consists of a hexagonal O–Mn–O trilayer adsorbed on Pt(111), i.e. similar to the previously found structure of FeO_{2-x} films [10].

In contrast to the MnO(19 × 1) films, the O-rich films readily react with CO. To illustrate this, Fig. 1c shows the HREEL-spectrum of the O-rich film after cycles of 200 L CO adsorption at 85 K and heating to 585 K. It is clear that the O-rich film is fully reduced to the (19 × 1) structure as identified by the reappearance of the characteristic 365 cm^{-1} and the disappearance of 583 and 721 cm^{-1} phonon bands.

3.2 CO Oxidation at Nearly Atmospheric Pressures

3.2.1 Structural Characterization

For reactivity studies, the MnO(19 × 1)–Pt(111) monolayer films were prepared by a Mn deposition at 300 K in UHV and subsequent annealing in 10^{-6} mbar O_2 at 700 K, which resulted in a LEED pattern displayed in Fig. 4a. This pattern results from superposition of three rotational domains each showing a (2.37 × 1) periodicity [15]. The same or newly deposited films oxidized at higher temperatures, ~850 K in this case, showed a much more complex LEED pattern (Fig. 4b). Yet structurally unidentified such films showed oxygen enrichment, resulting in a MnO_x ($x = 1.2$–1.4) composition measured by AES using the MnO-(19 × 1) structure for calibration.

The monolayer films prepared by oxidation at much higher O_2 pressures (10^{-4} mbar) at 700 K showed further enrichment in oxygen, as judged by AES (Fig. 5c), resulting in a close to MnO_2 compositional stoichiometry. The respective LEED pattern (Fig. 4c) is similar to that shown in Fig. 3a and as such it could be assigned to the

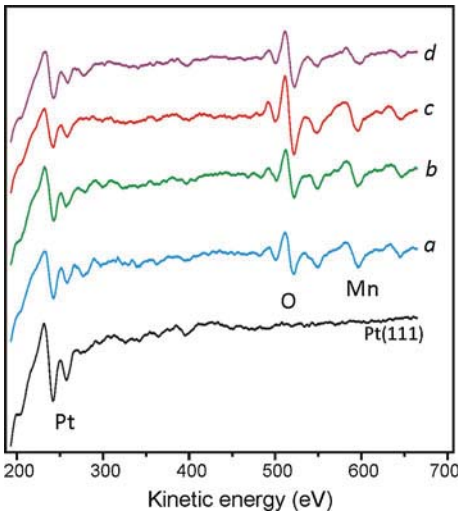

Fig. 5 Auger spectra of the same films (*a*–*d*) presented by LEED in Fig. 4 (see the preparation conditions therein). The spectrum for clean Pt(111) is shown for comparison

O–Mn–O trilayer structure. Another candidate for such O-rich films would be the "stripe" structure which, according to density functional theory (DFT) calculations [25], competes with the O-terminated unreconstructed bulk (111) face for the most stable structure at high chemical potentials of oxygen.

To examine structural transformations of the monolayer films under CO oxidation conditions at elevated pressures (further studied with GC in the HP reactor, see below), the "as prepared" films were exposed to 20 mbar O_2 at 450 K for 10 min. The resulting surfaces showed LEED very similar to those obtained on the "O-rich" films formed at 10^{-4} mbar O_2. In addition, the Auger spectrum (Fig. 5d) revealed a close to MnO_2 composition. It is noteworthy that the films did not dewet after HP treatments, as subsequent CO titration experiments did not reveal the Pt(111) surface.

Oxygen enrichment at high O_2 pressures is also observed in thermal desorption spectra. Figure 6 displays

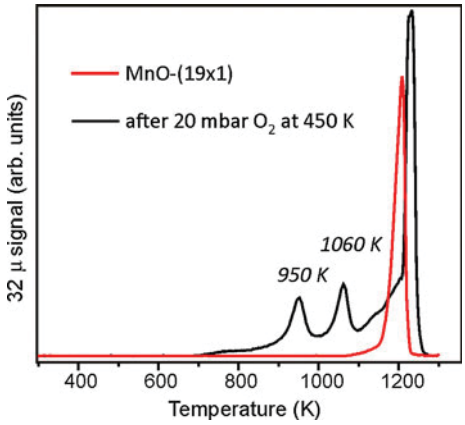

Fig. 6 Oxygen desorption from the monolayer MnO_x films on Pt(111): "as prepared" in 10^{-6} mbar O_2 at 850 K, and after exposure to 20 mbar O_2 at 450 K. The heating rate is 3 K s^{-1}

TPD profiles for 32 amu signal measured for the MnO(19 × 1)–Pt(111) film and the film further treated with 20 mbar O_2 at 450 K. The MnO-(19 × 1) film showed only one peak at 1200 K, thus indicating only one type of oxygen species in the film. In contrast, the O_2-treated film showed additional well-resolved signals at 950 and 1060 K indicating its sequential transformation to the "O-poor" film that ultimately decomposes at ~1230 K. The observed spectral changes are very similar to those shown in Fig. 3a measured in a different setup for a differently prepared "O-rich" sample. The peak centered at 950 K might be associated with oxygen atoms in the topmost layer of the O–Mn–O trilayer, like observed for a well-ordered O–Fe–O film on Pt(111) [10]. The peak at 1060 K, which obviously gains intensity for the sample prepared under high pressure conditions (compare to Fig. 3a), could be assigned either to another O-rich structure, coexisting with the above-proposed O–Mn–O structure, or to an intermediate structure formed upon heating during TPD. In principle, the former scenario would be in agreement with the DFT calculations predicting several stable structures for the MnO(111) surface at high chemical potential of oxygen [25]. Therefore, the oxidation conditions may affect the distribution of oxygen species in those films. Indeed, the peak centered at ~960 K in Fig. 3a exhibits a shoulder which is missing in Fig. 6. However, regardless of the nature of these peaks, close similarity between TPD profiles of the films treated at low (10^{-6} mbar) and high (20 mbar) pressures is quite remarkable. This finding suggests that the resultant structure is stable in a wide range of oxygen chemical potentials, although the films formed in the HP cell are poorly ordered as compared to the films prepared at low pressures and higher temperatures (compare Figs. 3b and 4d).

3.2.2 *Reactivity and Post-characterization*

The CO oxidation reaction was first examined under the same conditions as previously used for other oxide films studied in the group [7, 14, 26], i.e. in the mixture of 10 mbar CO and 50 mbar O_2 balanced by He to 1 bar at 450 K. Figure 7a shows kinetics of CO_2 production over a monolayer MnO film as well as of monolayer FeO(111) film and bare Pt(111) surface studied with the same setup for comparison. Clearly, the reactivity of MnO is significantly lower than of the FeO film and just slightly higher than of Pt(111). After ca. 15 min, the reaction over MnO slows down and then stops, indicating the catalysts deactivation.

Characterization of the post-reacted samples by LEED, AES and TPD revealed that the MnO_x films underwent severe dewetting which was accompanied in addition by carbon deposition, i.e. very similar to the reaction over the FeO films under O_2-lean conditions [7]. The spent MnO catalysts showed a well-known Pt(111)-c(4 × 2)CO pattern, and a substantial CO uptake by Pt(111) as measured by TPD. Heating of the sample to 600 K in UHV led to partial re-wetting of the Pt surface by the MnO-(19 × 1) film (not shown here).

In order to prevent dewetting, the reaction was further carried out at $CO:O_2 = 1:10$ while keeping the total reactant pressure of 60 mbar, i.e. 5.5 mbar CO and 54.5 mbar O_2, balanced by He to 1 bar. Note, that post-characterization by AES and TPD confirmed that the MnO_x film remains closed and showed all oxygen desorption features of the O-rich films shown in Fig. 6. Figure 7b clearly shows no deactivation and a much higher reactivity, although still lower than the FeO film. It is instructive to recall here that FeO(111) films on Pt(111) showed O_2 desorption at temperatures as low as 840 K [10], whereas the most weakly bound oxygen on the MnO film desorbs at 950 K, i.e. considerably higher. In this respect, it is noteworthy that closed ZnO films, which showed desorption at ~1070 K [14], were found essentially inert under the same conditions. Therefore, the O_2 desorption temperature, thus characterizing weakly bonded oxygen species in the film, can be used as a benchmark for activity in this reaction.

3.2.3 *High-Pressure XPS Study*

The monolayer films for in situ high pressure XPS studies were prepared by Mn deposition in 5×10^{-8} mbar O_2 at 300 K followed by oxidation in 10^{-6} mbar O_2 at 850 K. The "as prepared" films showed a LEED pattern virtually identical to that shown on Fig. 4b.

Exposure to 10^{-5} mbar at 300 K gives rise to additional O species that appear at ~530.8 eV as a shoulder at the high binding energy (BE) side of the main peak centered at

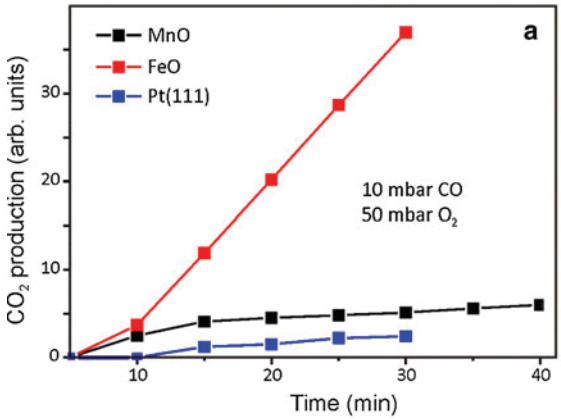

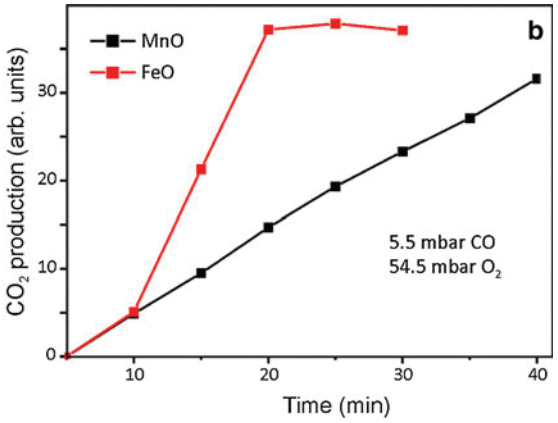

Fig. 7 Integrated CO_2 production over monolayer MnO_x film on Pt(111). Reaction conditions: 10 mbar CO, 50 mbar O_2, 450 K (**a**); 5.5 mbar CO, 54.5 mbar O_2, 450 K (**b**); He balance to 1 bar. Data for FeO(111)/Pt(111) and clean Pt(111), measured under the same conditions, are shown for comparison. Note that CO_2 production for the FeO film in **b** saturates due to the 100 % CO conversion after 20 min

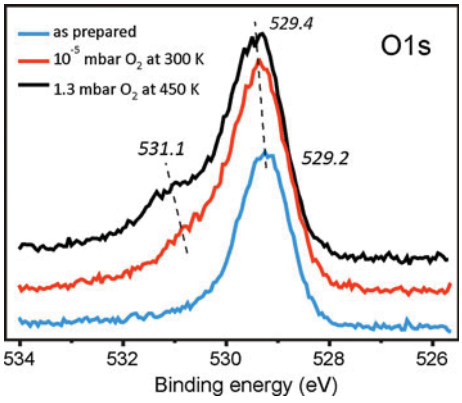

Fig. 8 XP-spectra of the O 1s region (hν = 750 eV) of a monolayer MnO_x film grown on Pt(111): as prepared (*blue*), after exposure to 10^{-5} mbar O_2 at 300 K (*red*), after exposure 1.3 mbar O_2 at 450 K (*black*). The spectra are offset for clarity

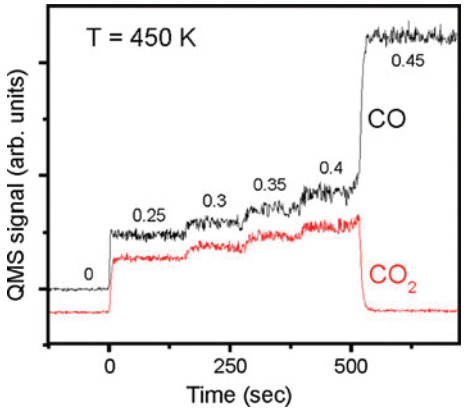

Fig. 9 CO oxidation kinetics upon stepwise increasing of a CO flow rate over a monolayer MnO_x film on Pt(111) at 450 K and constant O_2 flow of 5 ml/min. The CO flow rate (in ml/min) is indicated

529.2 eV (Fig. 8). The shoulder gains intensity and shifts to 531.1 eV after further treatment in 1.3 mbar of O_2 at 450 K in the HP cell. The main peak only slightly shifts from 529.2 to 529.4 eV upon oxidation. Concomitantly, the BE of Mn $2p_{3/2}$ core level shifts from 640.7 to 641.1 eV (not shown), thus indicating a higher oxidation state of Mn in the O-rich films, on average. Note that the Mn 2p spectrum is rather complex (as in several 3d transition metals) due to the multiplet splitting that renders quantitative analysis difficult [27].

Figure 9 displays the reaction kinetics monitored with QMS at stepwise increasing CO flow rate while keeping the O_2 flow rate constant (5 ml/min). It is clear that the CO_2 signal linearly responds to the changes in the CO concentration, thus suggesting a first order reaction for CO. Note that in the similar experiment over clean Pt(111) almost no response in CO_2 signal was observed. With increasing the CO:O_2 flow rates up to ~1:10, the activity drops down dramatically, indicating that the surface is deactivated. This is in agreement with the results of Fig. 7 showing that the CO:O_2 ratio is critical for the steady state reactivity.

The catalyst deactivation is accompanied by the substantial changes in the O 1s states. Figure 10 shows in situ XP spectra taken from the sample in active and deactivated states. The prominent shoulder to the main peak at 529.4 eV present on the active surface disappears on the deactivated surface. It cannot be restored by pure O_2 flow at the same 450 K, and the film remains almost inactive in a new reaction run. The deactivated surface readily adsorbs CO seen in the C 1s region at 286–287 eV (see Fig. S1 in the Supporting Information) and at ~532.7 eV in O 1s region that has tentatively been assigned to CO on Pt. Also, the spent catalyst exhibited clearly visible changes in the Mn $2p_{3/2}$ region (see Fig. S2). The two well-resolved peaks at 640.8 and 641.6 eV indicate very different Mn

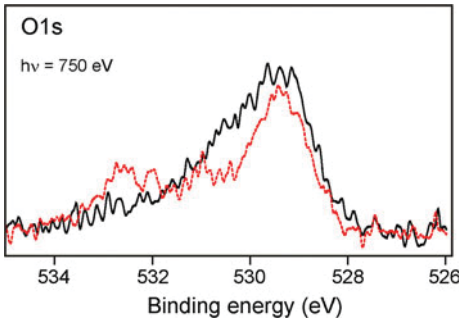

Fig. 10 In situ XP spectra of the O 1s region in a MnO_x/Pt(111) film measured under reaction conditions (450 K; $CO:O_2 = 1:10$; total pressure 1.3 mbar) in the active (*black solid line*) and deactivated (*red dashed line*) states. The feature at ~532.6 is assigned to the adsorbed CO

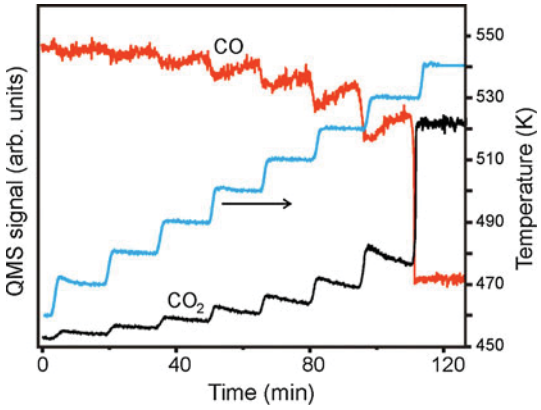

Fig. 11 QMS signals of CO (28 amu) and CO_2 (44 amu) in the flow reactor over a monolayer MnO_x film. A flow rate ratio is $CO:O_2 = 1:10$, a total pressure is ~1 mbar. The steady state regime at 450 K was first achieved prior to the following stepwise increasing the temperature. The CO and CO_2 traces were offset for clarity

coordination and, probably, oxidation states in the deactivated film. Taken together these results suggest that the film dewets under O_2-lean conditions, thus forming MnO_x particles on Pt(111), in agreement with the results presented above in Sect. 3.2.2.

Figure 11 shows the kinetics of CO oxidation (a total pressure ~1 mbar; a $CO:O_2$ flow ratio is 1:10) over the monolayer film at increasing reaction temperature following a steady state regime at 450 K. It appears that after 500 K the film underwent deactivation as can be concluded from CO concentration increase and CO_2 concentration decrease in the end of each temperature step. The remarkable gain of the reactivity at 530 K could be caused by morphological changes (dewetting), thus resulting in ill-defined MnO_x particles on Pt(111), which then dominates the reactivity. Adsorbed CO can be removed from the deactivated surface by oxygen treatment, but the catalyst did not regain its initial activity when the experiment was re-started at 450 K.

Therefore, the XPS results show that O_2 treatment of the monolayer MnO film at mbar pressure leads to a new O species which is characterized by about 1.8 eV higher BE of the O 1s core level as compared to the oxygen atoms initially present in the film. The additional O species could tentatively be assigned to the topmost O atoms in the O–Mn–O trilayer structure. The presence of these O species correlates well with enhanced reactivity of the film in low temperature CO oxidation.

4 Conclusions

The principal structure of monolayer MnO films grown on Pt(111) was studied by LEED, HREELS, AES, XPS and TPD at various chemical potential of oxygen (pressure, temperature). It is found that the monolayer MnO-(19 × 1) film prepared under UHV conditions readily transforms into "O-rich" films, which can be assigned, at least partially, to a O–Mn–O trilayer structure. The resulted films are fairly stable in a wide range of oxygen chemical potentials, although may show different degree of long-range ordering.

The monolayer MnO films were examined in the low temperature CO oxidation reaction at near atmospheric pressures. Reactivity studies revealed that the reaction rate over MnO films is higher than the Pt(111) support itself, but lower than FeO films studied under the same conditions. For stable catalytic performance MnO films required highly oxidizing reaction conditions ($CO:O_2 < 1:10$) to prevent film dewetting which causes irreversible catalyst deactivation.

The results show that the reactivity of MnO_x ultrathin films is governed by a weakly bonded oxygen species. Comparison with other [FeO(111) and ZnO(111)] films grown on the same Pt(111) shows, that desorption temperature of weakly bonded oxygen species can be used as a benchmark for activity in this reaction.

Acknowledgments The Swedish part of the work was supported by the Swedish Research Council (VR) and the Göran Gustafsson Foundation. Prof. J. Schnadt, Dr. J. Knudsen and the MAX-lab staff are gratefully acknowledged for their support. The FHI team acknowledges the support from the COST Action CM1104 "Reducible oxide chemistry, structure and functions". WW, SS, and SP gratefully acknowledge financial support by the Deutsche Forschungsgemeinschaft through SFB 762 "Functionality of Oxidic Interfaces". Finally, we thank Prof. L. Spiccia for fruitful discussions.

References

1. Freund H-J, Pacchioni G (2008) Oxide ultra-thin films on metals: new materials for the design of supported metal catalysts. Chem Soc Rev 37(10):2224–2242
2. Giordano L, Pacchioni G (2011) Oxide films at the nanoscale: new structures, new functions, and new materials. Acc Chem Res 44(11):1244–1252

3. Shaikhutdinov S, Freund H-J (2012) Ultrathin oxide films on metal supports: structure-reactivity relations. Annu Rev Phys Chem 63(1):619–633
4. Ackermann MD et al (2005) Structure and reactivity of surface oxides on Pt(110) during catalytic CO oxidation. Phys Rev Lett 95(25):255505
5. Gustafson J et al (2008) Sensitivity of catalysis to surface structure: the example of CO oxidation on Rh under realistic conditions. Phys Rev B 78(4):045423
6. Lundgren E et al (2006) Surface oxides on close-packed surfaces of late transition metals. J Phys: Condens Matter 18(30):R481
7. Sun YN et al (2009) Monolayer iron oxide film on platinum promotes low temperature CO oxidation. J Catal 266(2):359–368
8. Hellman A, Klacar S, Grönbeck H (2009) Low temperature CO oxidation over supported ultrathin MgO films. J Am Chem Soc 131(46):16636–16637
9. He YB et al (2008) Oxidation of Ir(111): from O–Ir–O trilayer to bulk oxide formation. J Phys Chem C 112(31):11946–11953
10. Sun Y-N et al (2010) The interplay between structure and CO oxidation catalysis on metal-supported ultrathin oxide films. Angew Chem 49(26):4418–4421
11. Rogal J, Reuter K, Scheffler M (2008) CO oxidation on Pd(100) at technologically relevant pressure conditions: first-principles kinetic Monte Carlo study. Phys Rev B 77(15):155410
12. Gustafson J et al (2004) Self-limited growth of a thin oxide layer on Rh(111). Phys Rev Lett 92(12):126102
13. Flege JI, Hrbek J, Sutter P (2008) Structural imaging of surface oxidation and oxidation catalysis on Ru(0001). Phys Rev B 78(16):165407
14. Martynova Y et al (2013) CO oxidation over ZnO films on Pt(111) at near-atmospheric pressures. J Catal 301:227–232
15. Hagendorf C et al (2008) Growth, atomic structure, and vibrational properties of MnO ultrathin films on Pt(111). Phys Rev B 77(7):075406
16. Sachert S et al (2010) Thickness dependent vibrational and electronic properties of MnO(100) thin films grown on Pt(111). Phys Rev B 81(19):195424
17. Rizzi GA et al (2001) An X-ray photoelectron diffraction structural characterization of an epitaxial MnO ultrathin film on Pt(111). Surf Sci 482–485(Part 2(0)):1474–1480
18. Müller F et al (2002) Epitaxial growth of MnO/Ag(001) films. Surf Sci 520(3):158–172
19. Li F et al (2009) Two-dimensional manganese oxide nanolayers on Pd(100): the surface phase diagram. J Phys: Condens Matter 21(13):134008
20. Nishimura H et al (2000) Surface structure of MnO/Rh(100) studied by scanning tunneling microscopy and low-energy electron diffraction. AVS, Seattle
21. Zhang L et al (2012) Growth and vibrational properties of MnOx thin films on Rh(111). Surf Sci 606(19–20):1507–1511
22. Schnadt J et al (2012) The new ambient-pressure X-ray photoelectron spectroscopy instrument at MAX-lab. J Synchrotron Radiat 19(5):701–704
23. Feulner P, Menzel D (1980) Simple ways to improve "flash desorption" measurements from single crystal surfaces. J Vac Sci Technol 17(2):662–663
24. Kostov KL et al (2013) Surface-phonon dispersion of a NiO(100) thin film. Phys Rev B 87(23):235416
25. Franchini C et al (2006) Density functional study of the polar MnO(111) surface. Phys Rev B 73(15):155402
26. Martynova Y et al (2012) Low temperature CO oxidation on ruthenium oxide thin films at near-atmospheric pressures. Catal Lett 142(6):657–663
27. Bagus PS, Ilton ES (2006) Effects of covalency on the p-shell photoemission of transition metals: MnO. Phys Rev B 73(15):155110